



MUSCULOSKELETAL PATHOLOGY

Excess Growth Hormone Triggers Inflammation-Associated Arthropathy, Subchondral Bone Loss, and Arthralgia



Sher B. Poudel,^{*} Ryan R. Ruff,[†] Gozde Yildirim,^{*} Manisha Dixit,^{*} Benoit Michot,[‡] Jennifer L. Gibbs,[‡] Silvana D. Ortiz,[§] John J. Kopchick,[§] Thorsten Kirsch,^{¶||} and Shoshana Yakar^{*}

From the Departments of Molecular Pathobiology^{*} and Epidemiology and Health Promotion,[†] David B. Kriser Dental Center, New York University College of Dentistry, New York, New York; the Department of Restorative Dentistry and Biomaterials Sciences,[‡] Harvard School of Dental Medicine, Boston, Massachusetts; the Department of Biomedical Sciences,[§] Edison Biotechnology Institute, Ohio University, Athens, Ohio; the Department of Orthopaedic Surgery,[¶] New York University Grossman School of Medicine, New York, New York; and the Department of Biomedical Engineering,^{||} New York University Tandon School of Engineering, New York, New York

Accepted for publication
February 10, 2023.

Address correspondence to
Shoshana Yakar, Ph.D.,
Department of Molecular
Pathobiology, New York Uni-
versity College of Dentistry,
David B. Kriser Dental Center,
345 E. 24th St., New York, NY
10010-4086.
E-mail: sy1007@nyu.edu.

Growth hormone (GH) is a key mediator of skeletal growth. In humans, excess GH secretion due to pituitary adenoma, seen in patients with acromegaly, results in severe arthropathies. This study investigated the effects of long-term excess GH on the knee joint tissues. One year-old wild-type (WT) and bovine GH (bGH) transgenic mice were used as a model for excess GH. bGH mice showed increased sensitivity to mechanical and thermal stimuli, compared with WT mice. Micro-computed tomography analyses of the distal femur subchondral bone revealed significant reductions in trabecular thickness and significantly reduced bone mineral density of the tibial subchondral bone—plate associated with increased osteoclast activity in both male and female bGH compared with WT mice. bGH mice showed severe loss of matrix from the articular cartilage, osteophytosis, synovitis, and ectopic chondrogenesis. Articular cartilage loss in the bGH mice was associated with elevated markers of inflammation and chondrocyte hypertrophy. Finally, hyperplasia of synovial cells was associated with increased expression of Ki-67 and diminished p53 levels in the synovium of bGH mice. Unlike the low-grade inflammation seen in primary osteoarthritis, arthropathy caused by excess GH affects all joint tissues and triggers severe inflammatory response. Data from this study suggest that treatment of acromegalic arthropathy should involve inhibition of ectopic chondrogenesis and chondrocyte hypertrophy. (*Am J Pathol* 2023, 193: 829–842; <https://doi.org/10.1016/j.ajpath.2023.02.010>)

Arthropathy is highly prevalent in patients with acromegaly¹ [bearing pituitary adenoma that releases excess growth hormone (GH) to the circulation] and persists despite biochemical control [ie, normalization of insulin-like growth factor-1 (IGF-1) levels in serum].¹ Painful arthropathy is perceived as the major contributor to reduced quality of life in patients with acromegaly.¹ However, treatment of this comorbidity provides only symptomatic relief (physiotherapy and consumption of pain and anti-inflammatory agents) and does not prevent disease progression.

Secondary osteoarthritis (OA), seen in patients with acromegaly, does not resemble injury- or aged-induced

primary OA. Although age- or injury-induced OA is characterized by decreased joint space, thinning of the articular cartilage, and absent or mild osteophytosis, acromegaly-associated OA is typified by increased joint space, thickening and hypertrophy of the articular cartilage, and severe osteophytosis.² Therefore, treatments that may apply to age- or injury-induced OA may not be relevant to acromegalic-associated OA. Additionally, it is plausible that the molecular mechanism driving secondary OA in patients with

Supported by NIH grants R01AG056397 (S.Y.) and S10 OD010751-01A1 for micro-computed tomography.

Disclosures: None declared.

acromegaly are different from those driving primary or injury-induced OA.

Clinical studies describe two phases of acromegalic arthropathy. The initial phase is characterized by cartilage hypertrophy with laxity of the periarticular ligaments, leading to impaired mechanical force distribution that results in morphologic changes in the joint.² During this phase, an increased joint space is evidenced radiographically. It is believed that at this early phase, arthropathy is reversible or that its progression can be controlled.³ The second phase of the disease occurs even when biochemical control is achieved. This stage is typified by severe osteophytosis, increased cartilage thickness, and edema. Arthropathy at this stage becomes irreversible.

Progression of OA affects all tissues of the joint and is characterized by the structural and functional deterioration of the articular cartilage (AC), subchondral and periarticular bones, synovial membrane, ligaments, and adjacent muscle tissues.⁴ Degeneration of the AC, release of breakdown components of the extracellular matrix, and dysfunction of chondrocyte accelerate the progression of OA.^{5,6}

GH plays important roles in maintaining the AC homeostasis, including stimulation of progenitor cell proliferation, differentiation,⁷ and extracellular matrix mineralization.⁸ GH acts on chondrocytes of the AC directly through binding to the GH receptor. GH receptor actions can be mediated by local production of IGF-1 or independent of IGF-1.⁹ Herein, the bovine GH (bGH) transgenic mice were used as a model of excess in GH and IGF-1, to study how long-term exposure to extreme levels of GH affect the integrity of the AC. Only three studies using the bGH mice^{10,11} described the effects of excess GH/IGF-1 on the articular cartilage (AC) of the knee joint. These studies focused on two-dimensional analyses of chondrocyte hypertrophy in the AC,^{10–12} but did not address osteophytosis, which is central to acromegalic arthropathy,² and did not study other tissues of the joint. The current study focused on the AC, synovial membrane, three-dimensional (3D) analysis of subchondral bone (SCB) in femur and tibia, and the SCB-plate in tibia of male and female mice at 1 year of age. Histologic and immunohistochemistry findings were related to SCB morphologic traits obtained by micro-computed tomography (micro-CT).

Materials and Methods

Mice

All procedures involving mice were reviewed and approved by the Institutional Animal Care and Use Committee of the NYU School of Medicine (New York, NY). Generation of the bGH transgenic mice on a C57BL/6J genetic background was previously described.¹³ Male bGH transgenic mice were mated with wild-type (WT) females, and the offspring (which were WT or hemizygote bGH mice) were randomly allocated into cages according to their sex. Note

that female bGH mice are infertile; thus, the bGH transgene is always paternally transmitted, and all offspring are hemizygote. Mice were housed two to five animals per cage in a facility with 12-hour light/dark cycles and free access to food and water. Mice were studied at 12 months of age.

Mechanical Sensitivity

Mice were placed individually in a small transparent plastic testing box (3 × 3 × 4 inches) with ventilation holes on an elevated wire mesh. Before any stimulation session, mice were allowed to acclimate to the testing environment for 30 minutes. Then, mechanical sensitivity was determined using a graded series of seven von Frey filaments (Stoelting, Wood Dale, IL) that produced a force of 0.04, 0.07, 0.16, 0.4, 0.6, 1.0, and 2.0 g. The stimuli were applied on the plantar surface of the hind paw, and the 50% paw withdrawal threshold was calculated using the up and down method, as previously described.¹⁴ A response was considered positive if the animal exhibited brisk paw withdrawal, paw licking, or paw shaking.

Thermal Sensitivity

Mice were placed individually in a small transparent plastic testing box (3 × 3 × 4 inches) with ventilation holes on a glass surface. After 30 minutes of acclimation to the testing environment, thermal sensitivity was measured using a Hargreaves' thermal stimulator (Hargreaves' Apparatus; University of California, San Diego, La Jolla, CA). The radiant heat source was applied to the plantar surface of the hind paw until an aversive reaction was observed or up to 15 seconds to avoid tissue damage. A positive aversive response was defined as brisk hind paw withdrawal, hind paw lick, or hind paw shaking. The paw withdrawal latency was calculated from six trials per animal with at least a 5-minute interval between each test.

Micro-Computed Tomography

Micro-CT of the knee joints was done in accordance with the American Society for Bone and Mineral Research guidelines.¹⁵ Intact femur and tibia, including the knee joint, were scanned using a high-resolution SkyScan micro-CT system (SkyScan 1172; Bruker, Kontich, Belgium) containing a 10-megapixel digital detector set at a 10-W energy level (100 kV and 100 μ A), with a 0.5-mm aluminum filter with a 9.7- μ m image voxel size. Subchondral bone parameters were taken in the distal femur below the AC, avoiding cortical bone, and included bone volume fraction [bone volume/tissue volume (BV/TV); %], trabecular thickness (Tb.Th; mm), trabecular number (1/mm), and bone mineral density (BMD; mg/mL). Subchondral bone plate (SCBP) thickness and BMD were measured at the proximal tibia. Data reconstruction was done using NRecon software version 1.7.4.2 (Bruker), and data analysis was performed using CTAn software version 1.18.4.0 (Bruker). Three-dimensional

images were obtained using CT Vox software version 3.30r1403 (Bruker).

Histology

Following dissection, knee joints were decalcified in 10% EDTA for 4 to 5 weeks, dehydrated using a graded alcohol series and xylene, and processed for paraffin embedding and sectioning. Safranin-O-red staining was used for scoring the AC of the knee joint, including the presence and maturation stage of osteophytes as well as the ectopic chondrogenesis and ossification. Hematoxylin and eosin staining was used to score inflammation of synovial membrane and overall morphology.

Osteoarthritis Score

Cartilage damage at medial and lateral tibiofemoral joints was evaluated by two blinded observers (S.B.P. and T.K.) using the Osteoarthritis Research Society International scoring system.¹⁶ Loss of cartilage proteoglycan was scored by safranin-O-red; normal staining of noncalcified cartilage was scored 0; loss of safranin-O-red staining without structural changes was scored 0.5; small fibrillations without loss of cartilage were scored 1; vertical clefts down to the layer immediately below the superficial layer and some loss of surface lamina were scored 2; vertical clefts/erosion to the calcified cartilage extending to <25% of the articular surface were scored 3; vertical clefts/erosion to the calcified cartilage extending to 25% to 50% of the articular surface were scored 4; vertical clefts/erosion to the calcified cartilage extending to 50% to 75% of the articular surface were scored 5; and vertical clefts/erosion to the calcified cartilage extending to >75% of the articular surface were scored 6. Osteophyte maturity was scored 0 when no osteophytes were detected; 1 when osteophytes were composed of a precartilaginous lesion; 2 when osteophytes were composed predominantly of cartilage; 3 when osteophytes were composed of mixed cartilage and bone; and 4 when osteophytes were composed predominantly of bone.¹⁷ Synovitis was scored from hematoxylin and eosin-stained sections.^{18–20} Briefly, the thickness of the synovial cell lining layer and the cell density within this layer were scored from 0 to 3, with 0 being the thinnest synovial cell lining layer and low cell density (one to two cell layers), 1 with three to five cell layers, 2 with six to eight cell layers, and 3 being the thickest synovial cell lining layer (more than eight layers) and high cell density. Ectopic chondrogenesis was scored 0 when it was undetectable, 1 when it was found in the synovium and/or the capsule, and 2 when it extended into the surrounding ligament and/or musculature.²¹

Immunohistochemistry

Following deparaffinization and rehydration, the tissue sections were treated with citrate-based antigen unmasking

solution (H-3300; Vector Laboratories, Inc., Newark, CA). Then, endogenous peroxidase activity was inactivated by Bloxall endogenous blocking solution (SP-6000; Vector Laboratories, Inc.). After blocking using the protein block solution (ab64226; Abcam, Waltham, MA), the sections were incubated overnight with the primary antibodies at 4°C, stained by rabbit-specific horseradish peroxidase/diaminobenzidine (avidin-biotin complex) detection kit (PK-4001/SK-4100; Vector Laboratories, Inc.) and counterstained by hematoxylin (Sigma, St. Louis, MO). The images were acquired by DMRXE universal microscope with objective imaging gigapixel montaging workstation (Leica Biosystems, Deer Park, IL) and analyzed by Fiji ImageJ (ImageJ version 1.53t; NIH, Bethesda, MD; <https://imagej.nih.gov/ij/download.html>, last accessed August 22, 2022). For immunohistochemistry, primary antibodies were against CD86 (1:150; bs-1035R; Bioss Inc., Woburn, MA), inducible nitric oxide synthase (iNOS; 1:300; PA3030A; Invitrogen, Waltham, MA), Ki-67 (1:150; PA5-19462; Invitrogen), matrix metalloproteinase 13 (MMP13; 1:50; 18165-1-AP; Proteintech, Rosemont, IL), nucleotide oligomerization domain (NOD)-like receptor-pyrin domain-containing 3 (NLRP3; 1:300; PA5-88709; Invitrogen), p53 (1:50; ab131442; Abcam), Runt-related transcription factor 2 (RUNX2; 1:100; NBPI-77461; Novus Biologicals, Englewood, CO), sex-determining region Y (SRY) box transcription factor 9 (SOX9; 1:50; AB5535; MilliporeSigma, Burlington, MA), and type X collagen (1:150; PA5-115039; Invitrogen).

Statistical Analysis

Individual descriptive statistics (eg, means, medians, and interquartile ranges) were computed overall and by group for each outcome. To allow for dependency in response variables, all outcomes described were first analyzed using one-factor nonparametric multivariate analysis of variance with permutation tests (10,000 permutations per outcome). Significant variables identified in this stage were subsequently analyzed using two-factor aligned ranks transformation analysis of variance. Included factors were genotype and sex (and the genotype-sex interaction). Individual *P* values for overall *F*-tests were adjusted using the method of Yoav Benjamini²² to control for the family-wise error rate. *P* values for the genotype-sex contrast were further adjusted using the Bonferroni method. Data analysis was conducted in R version 4.1.3 (<https://www.r-project.org>).

Results

Excess GH Associates with Arthralgia

At 1 year of age, bGH mice showed a significant increase in body weight of 45% and 77% in male and female mice, respectively (Figure 1A), whereas femoral length had a significant increase of 15% and 19% in male and female

mice, respectively (Figure 1B). Increases in body weight and femur length were associated with a significant increase in serum IGF-1 levels (Figure 1C). Aged bGH mice showed decreased cage activity, a typified pain-related behavior, that was evidenced as early as 3 months of age. To assess pain sensitivity, the manual von Frey test was used, which is the gold standard for determining mechanical thresholds indicated in mice by paw withdrawal. Increased sensitivity to mechanical stimulation (evidenced by reduced pressure required to exert a response) was detected in both male and

female bGH mice compared with that in controls (Figure 1D). However, there was no significant sex × genotype interaction when tested for mechanical sensitivity. Thermal sensitivity was tested using Hargreaves test (Figure 1E). Male bGH mice exhibited significantly increased thermal sensitivity (evidenced by reduced latency required to exert a response), whereas female bGH mice showed increased thermal sensitivity that did not reach significance. There was no significant sex × genotype interaction when tested for thermal sensitivity.

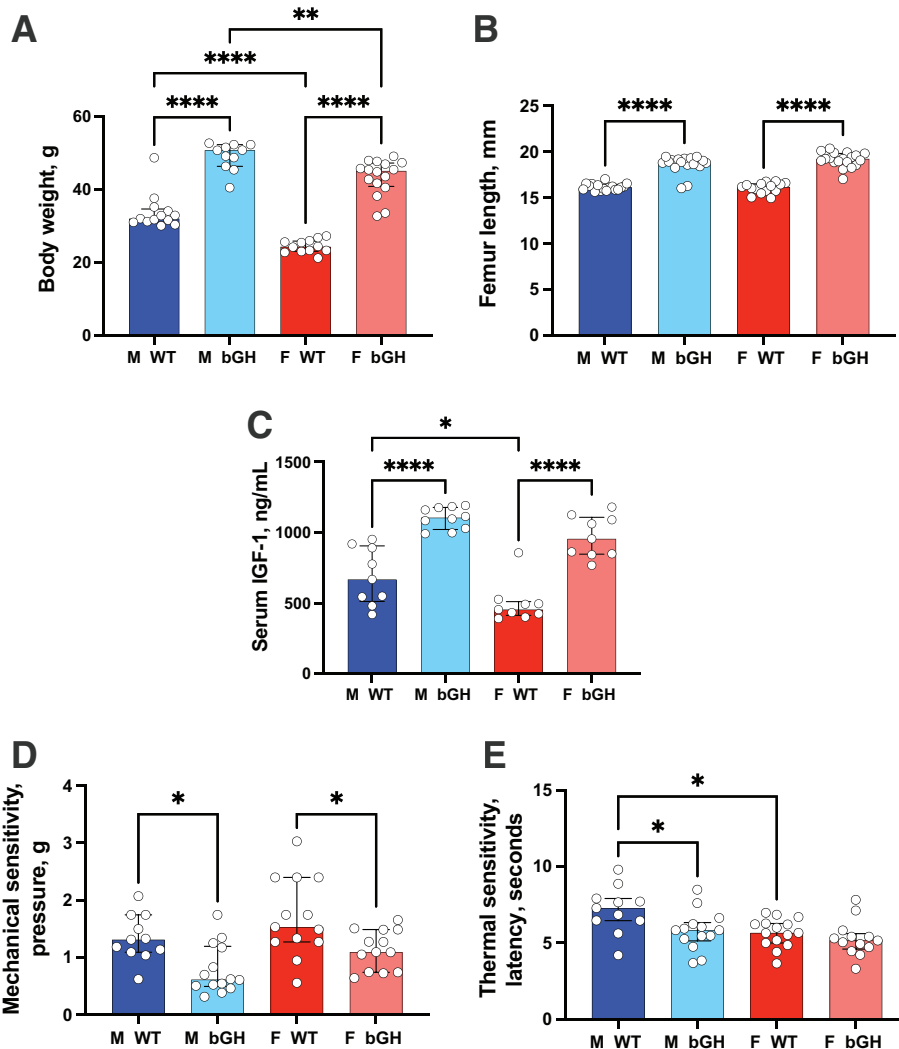


Figure 1 Osteoarthritis-associated arthralgia in bovine growth hormone (bGH) mice. **A–C:** One-year-old bGH mice exhibit increased body weight (**A**) and increased femur length (**B**), associated with significant increases in serum insulin-like growth factor-1 (IGF-1) levels (**C**), compared with age-matched wild-type (WT) mice [body weight: male (M) WT, *n* = 13; M bGH, *n* = 11; female (F) WT, *n* = 12; and F bGH, *n* = 16; femur length: M WT, *n* = 17; M bGH, *n* = 17; F WT, *n* = 15; and F bGH, *n* = 19; and serum IGF levels: M WT, *n* = 9; M bGH, *n* = 10; F WT, *n* = 9; and F bGH, *n* = 9]. **D:** von Frey test: mice were placed individually in a small cage on an elevated wire mesh. A monofilament was applied perpendicularly to the plantar surface of the hind paw until it buckles, delivered at a constant predetermined force (0.04 to 2.0 g) for 2 to 5 seconds. Both male and female bGH mice responded to a lower pressure, indicating increased sensitivity (M WT, *n* = 11; M bGH, *n* = 14; F WT, *n* = 13; and F bGH, *n* = 13). **E:** Hargreaves’ test: the latency to respond to a thermal stimulus applied to the paw was determined by the time it takes for the mouse to withdraw the hind paw from the heat source and/or lick the hind paw. bGH male mice showed a significant reduction in the latency of a nociceptive behavior (M WT, *n* = 11; M bGH, *n* = 14; F WT, *n* = 15; and F bGH, *n* = 13). Data presented as median ± IQR (**A–E**). **P* < 0.05, ***P* < 0.01, and *****P* < 0.0001.

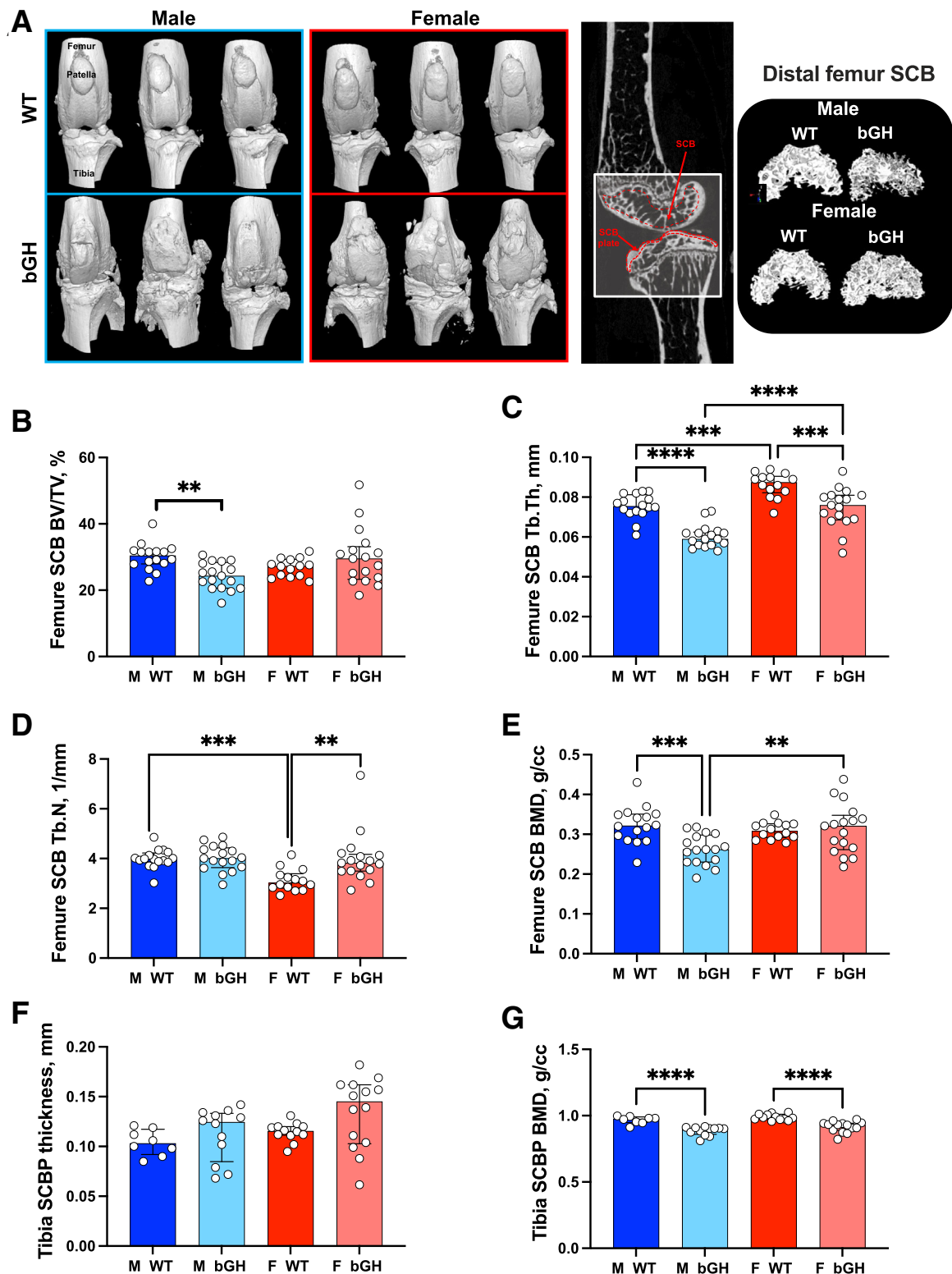


Figure 2 Excess growth hormone (GH) impairs the morphology of the femur subchondral bone (SCB) and significantly reduces the tibia SCB plate bone mineral density (BMD). **A**: Micro-computed tomography (micro-CT) three-dimensional (3D) images of the knee joint from 1-year-old male and female wild-type (WT) and bovine GH (bGH) mice, along with 3D reconstruction of the distal femur SCB, and two-dimensional images indicating the region of interest. **B–E**: Parameters assessed by micro-CT at the distal femur SCB included bone volume/total volume (BV/TV; **B**), trabecular thickness (Tb.Th; **C**), trabecular number (Tb.N; **D**), and SCB bone mineral density (**E**). **F** and **G**: SCB plate (SCBP) thickness (**F**) and SCBP bone mineral density (**G**) were determined at the proximal tibia. Data presented as median \pm IQR (**B–G**). $n = 16$ male (M) WT (**B–G**); $n = 17$ M bGH and female (F) bGH (**B–G**); $n = 14$ F WT (**B–G**). $**P < 0.01$, $***P < 0.001$, and $****P < 0.0001$. cc, cubic centimeter.

Excess GH Impairs the Morphology of the Femur Subchondral Bone and Significantly Reduces the Mineral Density of the Tibia Subchondral Plate

Micro-CT, followed by 3D reconstructions of the knee (Figure 2), in 1-year-old WT and bGH mice indicated an impaired joint morphology with multiple bone spurts (osteophytes) evidenced at the distal femur and proximal tibia (Figure 2A). A detailed analysis of the SCB compartment was achieved by micro-CT. Significant sex-dependent microstructural differences were observed between WT and bGH mice. Male bGH mice showed significant reductions in SCB volume (BV/TV, with $P = 0.003$ for sex \times genotype interaction) (Figure 2B), decreased SCB Tb.Th (Figure 2C) without changes in trabecular number (Figure 2D), and significantly reduced SCB mineral density (BMD, with $P = 0.012$ for sex \times genotype interaction) at the distal femur (Figure 2E). Decreases in BV/TV and Tb.Th in bGH male mice were associated with increased tartrate-resistant acid phosphatase staining in the SCB compartment (Supplemental Figure S1). Female bGH mice showed significantly reduced Tb.Th (Figure 2C), but, unlike male bGH mice, trabecular number was increased in female bGH mice, with $P = 0.014$ for sex \times genotype interaction (Figure 2D), and led to similar SCB BV/TV (Figure 2B). SCB mineral density was not affected in female bGH mice (Figure 2E). SCBP is a thin cortical plate subjacent to calcified cartilage, which is a penetrable porous structure. SCBP in the proximal tibia was analyzed using micro-CT. Both male and female bGH mice showed increases in the proximal tibia SCBP plate thickness compared with WT mice (Figure 2F), but this did not reach significance because of large variability. Interestingly, both male and female bGH mice showed significant decreases in SCBP BMD (Figure 2G).

Excess GH is Associated with Severe AC Deformity and Ectopic Chondrogenesis

Knee joints of 1-year-old WT and bGH mice were characterized histologically using safranin-O-red staining and scored according to the Osteoarthritis Research Society International scoring system in the medial (Supplemental Figure S2, A and B) and lateral (Supplemental Figure S2, C and D) sides of femoral condyle and tibial plateau (Figure 3A). bGH male and female mice showed significantly higher cumulative scores in femur and tibia (Figure 3B), which deferred significantly in the medial side of the joint (Supplemental Figure S2, A and B). Increased Osteoarthritis Research Society International scores were also evidenced in the lateral part of the joints in bGH compared with WT mice, but they reached significance only in the lateral tibia of bGH males (Supplemental Figure S2D). More importantly, both male and female bGH mice, but not WT mice, displayed hypertrophic cartilage (Figure 3C), which was associated with increased type

X collagen staining (Figure 3D and Supplemental Figure S3A). Interestingly, expression of the transcription factor SOX9, which is required for protecting the AC from degradation and prevents chondrocyte dedifferentiation to osteoblast-like cells,²³ was significantly decreased in bGH mice of both sexes (Figure 3E and Supplemental Figure S3B). The levels of RUNX2 transcription factor were significantly increased, which played a role in hypertrophic differentiation and catabolic processes in AC of bGH mice in both sexes (Figure 3F and Supplemental Figure S3C).

The 3D reconstruction of micro-CT images of the knee joint revealed that bGH mice developed osteophytosis (Figure 2A). Osteophytes are fibrocartilage-capped bony outgrowths and are a common feature of osteoarthritis. Scoring of osteophyte size and maturity using the safranin-O-red-stained sections (Figure 4A) showed increases in cumulative scores of osteophyte formation in male and female bGH mice compared with those in WT mice (Figure 4B). Osteophyte formation in femur (Supplemental Figure S4, A and B) and tibia (Supplemental Figure S4, C and D) in the medial side of the joint significantly increased in bGH male and female mice. In the lateral joint, significantly increased osteophyte formation was evidenced in tibia of both sexes, whereas it was increased in the femur of bGH females only.

Finally, severe ectopic chondrogenesis and ossification of the joint (Figure 4C) were found in bGH mice of both sexes at the medial and lateral sides of the joint (Figure 4D and Supplemental Figure S4, E and F). A total of 100% of male and female bGH mice exhibited ectopic chondrogenesis, whereas only 33% and 50% of WT male and female mice, respectively, developed ectopic chondrogenesis, which was not as severe as that observed in the bGH mice.

Excess GH is Associated with Increased Levels of Inflammatory Markers in the AC

Chondrocyte inflammation and MMP activities accelerate cartilage degradation and promote OA progression.^{24,25} Immunohistochemistry was used to determine the role of excess GH in chondrocyte expression of inflammatory proteins. Significantly increased levels of iNOS, one of the major inflammatory mediators in OA pathogenesis,²⁶ were found in AC chondrocytes of bGH male and female mice (Figure 5, A and E, and Supplemental Figures S5, A and B, and S6, A and B). NLRP3 inflammasome (also called cryopyrin) is an intracellular protein primarily found in white blood cells and chondrocytes. NLRP3 has been recognized as a major inflammatory marker associated with the pathogenesis of arthropathy, cartilage degeneration, and synovitis.²⁷ Significantly increased levels of NLRP3 immunopositive chondrocytes were observed in male and female bGH compared with those in WT mice (Figure 5, B and E, and Supplemental Figures S5, C and D, and S6, C and D). MMP13, a key enzyme in the cleavage of type II

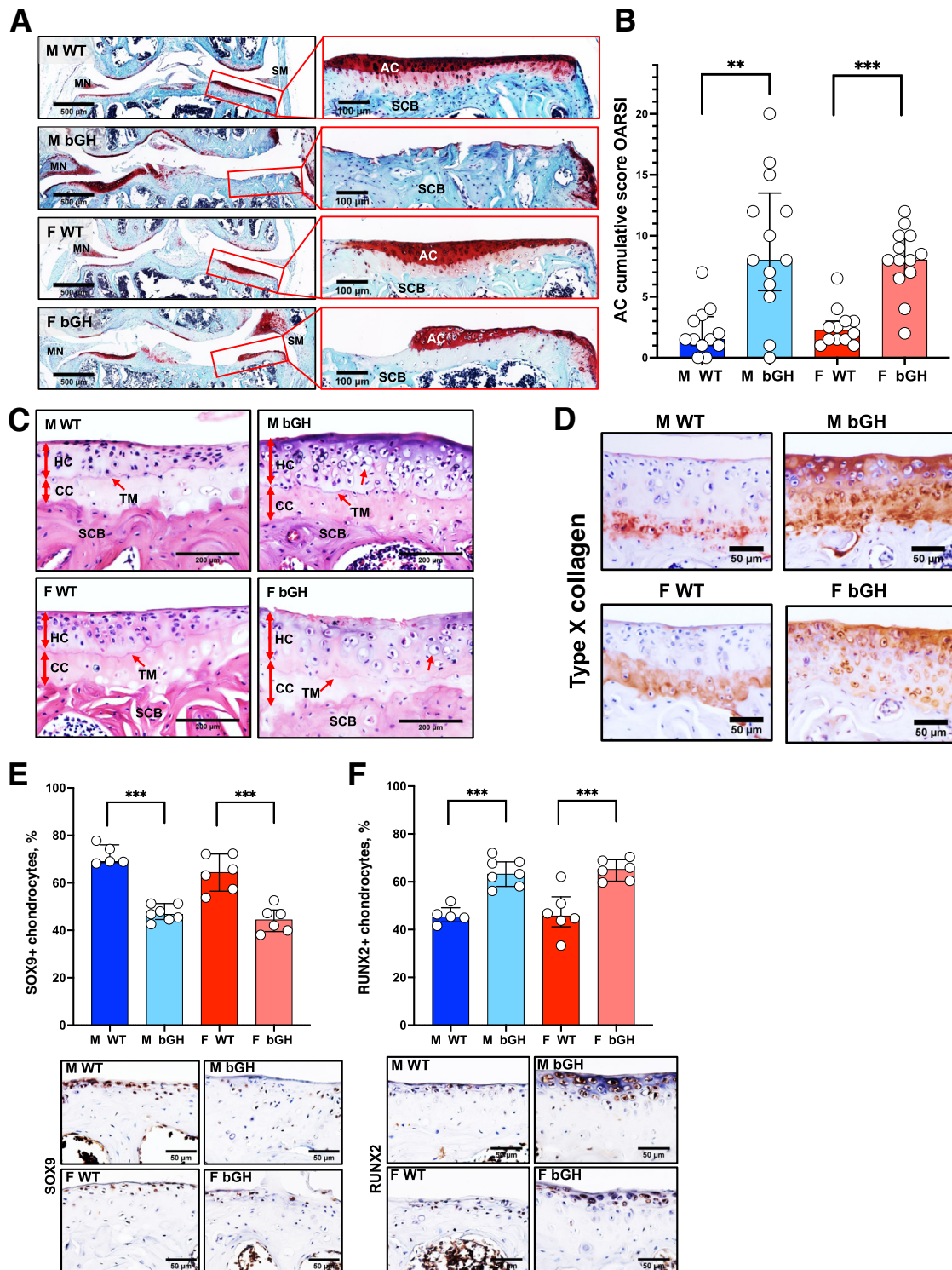


Figure 3 Excess growth hormone (GH) leads to the development of osteoarthritis. **A:** Representative safranin-o-red–stained sections of the knee joint. Cartilage loss was scored according to the Osteoarthritis Research Society International (OARSI) system. **B:** Presented are cumulative OARSI scores of the femur and tibia [male (M) wild type (WT), $n = 12$; M bovine GH (bGH), $n = 13$; female (F) WT, $n = 11$; and F bGH, $n = 13$]. **C:** Representative images of coronal sections of the tibial plateau stained with hematoxylin and eosin. **Red arrows** indicate calcified cartilage (CC), hyaline cartilage (noncalcified; HC), tide mark (TM), subchondral bone (SCB), and hypertrophic chondrocytes. **D:** Presented are immunohistochemistry–stained images of type X collagen in articular cartilage (AC). **E** and **F:** Expression levels of sex-determining region Y (SRY) box transcription factor 9 (SOX9; **E**) and Runt-related transcription factor 2 (RUNX2; **F**) were assessed by immunohistochemistry. Presented are percentages of positive AC chondrocytes (at the distal femur and tibia) alongside representative immunostained images of coronal sections of the tibial plateau (M WT, $n = 5$; M bGH, $n = 7$; F WT, $n = 6$; and F bGH, $n = 6$). Data presented as median \pm IQR (**B**, **E**, and **F**). $**P < 0.01$, $***P < 0.001$. Scale bars: 500 μm (**A**, left panels); 100 μm (**A**, right panels); 200 μm (**C**); 50 μm (**D–F**). MN, meniscus; SM, synovial membrane.

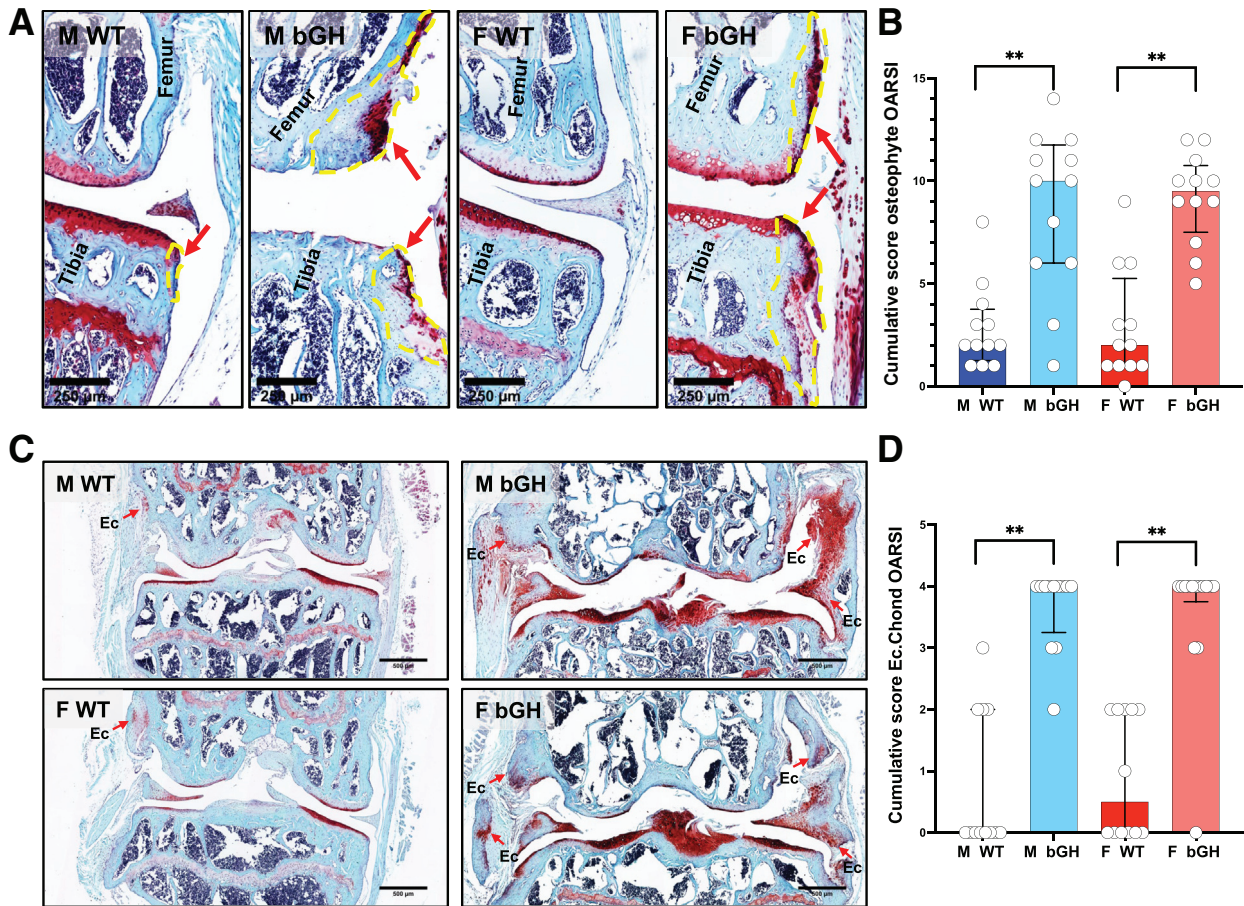


Figure 4 Excess growth hormone (GH) associates with increased osteophytosis and ectopic chondrogenesis (Ec. Chond). **A:** Osteophytosis was quantified according to the Osteoarthritis Research Society International (OARSI) scoring system from safranin-o-red–stained sections. **Yellow lines** and **red arrows** define osteophytes. **B:** Presented are cumulative scores of osteophyte formation in the distal femur and proximal tibia. **C:** Ectopic chondrogenesis was scored from safranin-o-red–stained sections. **Red arrows** point to areas of ectopic chondrogenesis. **D:** Presented are cumulative scores of ectopic chondrogenesis at all the knee joint tissues. Bovine growth hormone (bGH) mice showed increases in ectopic chondrogenesis at all the knee joint tissues. Data presented as median ± IQR (**B** and **D**). $n = 12$ male (M) wild type (WT), M bGH, and female (F) WT (**B** and **D**); $n = 13$ F bGH (**B** and **D**). $**P < 0.01$. Scale bars: 250 μm (**A**); 500 μm (**C**).

collagen, plays a pivotal role in degradation of the AC extracellular matrix.²⁸ As expected, the significantly increased MMP13-positive chondrocytes were seen in male and female bGH mice (Figure 5, C and E, and Supplemental Figures S5, E and F, and S6, E and F).

Finally, GH is known to inhibit the tumor suppressor p53 protein.²⁹ Significant inhibition of p53 in the AC of bGH mice (Figure 5D and Supplemental Figures S5, G and H, and S6, G and H) was seen, which was not associated with increased Ki-67, a marker of proliferation, in chondrocytes (Supplemental Figure S6, I–L). Instead, significant increases in type X collagen, a marker of chondrocyte hypertrophy, was seen in the AC of both male and female bGH mice compared with the respective WT mice (Figure 3D and Supplemental Figure S3).

Excess GH is Associated with Severe Synovitis

Hematoxylin and eosin staining of the synovium (Figure 6A) showed thickening of the synovial membrane in

both male and female bGH compared with WT mice (Figure 6B and Supplemental Figure S7, A and B). This was evidenced by increased cell density in the synovial membrane of the bGH mice (Figure 6C and Supplemental Figure S7, C and D), indicating that excess bGH led to hyperplasia and likely inflammation of the synovium. Immunohistochemical staining revealed increases in inflammatory markers, including CD86 (Figure 6D and Supplemental Figures S7E and S8A), iNOS (Figure 6E and Supplemental Figures S7F and S8B), and NLRP3 (Figure 6F and Supplemental Figures S7G and S8C) in both medial and lateral synovial membrane, that were associated with increased Ki-67 proliferation marker in the synovium (Figure 6G and Supplemental Figures S7H and S8D).

Discussion

bGH mice exhibit excess levels of GH and IGF-1 in serum and tissues.³⁰ These mice exhibit reduced lifespan (12 to 15 months of age), increased neoplasia, increased

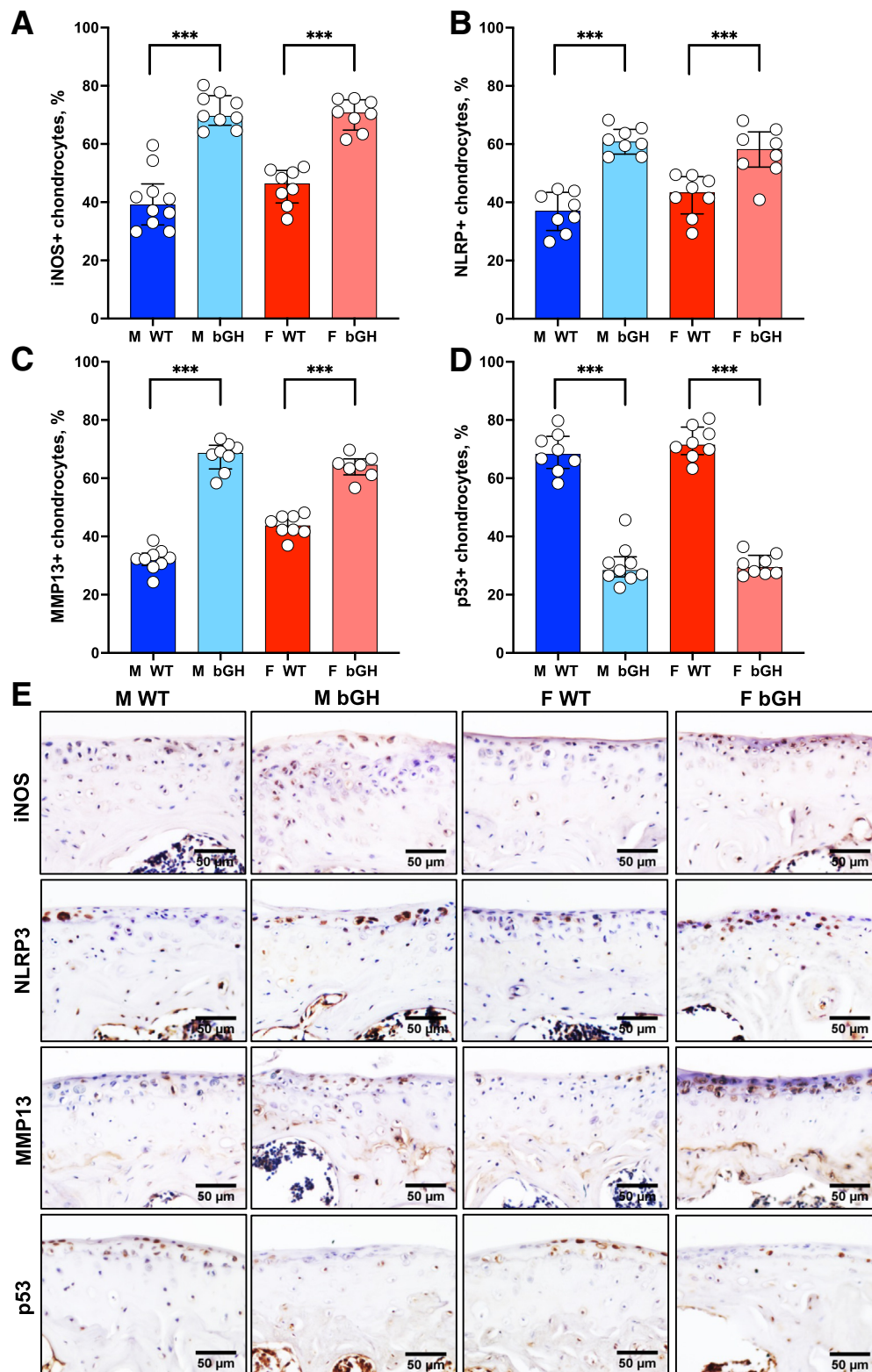


Figure 5 Excess growth hormone (GH) is associated with increased chondrocyte expression of inflammatory markers (medial side of the knee joint) and inhibited tumor suppressor p53 expression. Expression of inflammatory markers was assessed by immunohistochemistry. **A–D:** Presented are percentages of positive articular cartilage (AC) chondrocytes (at the distal femur and tibia) to the following markers: inducible nitric oxide synthase [iNOS; male (M) wild type (WT), $n = 10$; M bovine GH (bGH), $n = 9$; female (F) WT, $n = 8$; and F bGH, $n = 8$; **A**], nucleotide oligomerization domain (NOD)-like receptor-pyrin domain-containing 3 (NLRP3; $n = 8$ in each group; **B**), matrix metalloproteinase 13 (MMP13; M WT, $n = 9$; M bGH, $n = 8$; F WT, $n = 8$; and F bGH, $n = 7$; **C**), and p53 (M WT, $n = 8$; M bGH, $n = 9$; F WT, $n = 8$; and F bGH, $n = 8$; **D**). **E:** Representative immunohistochemistry images of the AC. Data presented as median \pm IQR (**A–D**). $***P < 0.001$. Scale bars = 50 μm (**E**).

inflammation, and metabolic abnormalities.³¹ Herein, radiographic imaging (micro-CT) and 3D reconstructions of 1-year-old bGH knee joints revealed significant alterations in the morphology of the SCB at the distal femur and proximal tibia. Histologic assessments showed that both male and female bGH mice presented with severe OA, hypertrophic chondrocytes in the AC with multiple OA lesions, severe osteophytosis, synovitis, and ectopic chondrogenesis in both medial and lateral sides of the joint, which seemed unrelated to the gait-loading principle. Immunohistochemistry revealed that excess GH triggered inflammation in all joint tissues, including the AC and the synovial membrane in both medial and lateral sides of the joint. Furthermore, immunohistochemistry indicated increases in type X collagen and RUNX2 immunostaining, possibly indicating dedifferentiation of AC chondrocytes in the bGH joints. Finally, OA in bGH mice was associated with arthralgia, evidenced by sensitivity to mechanical (von Frey assay) or thermal (Hargreaves test) stimuli.

There is an intimate physical relationship between SCB and the AC, forming a bone-cartilage unit that allows interactions between osteoclasts, osteoblasts, and chondrocytes.³² The nature of this cross talk is not well understood. However, there are indications that osteoclastic activity in SCB can initiate a cascade of inflammatory events that aggravates OA.³² Indeed, early stages of primary OA are characterized by enhanced SCB turnover, where the trabeculae become thinner and porous because of increased osteoclast activity, the SCBP thickens, and the cartilage undergoes degradation, a gradual process that progresses to late stages of OA. In fact, enhanced SCB remodeling due to microdamage was reported in horses.³³ Secondary OA, seen in subjects with acromegaly or in the bGH mice, is partially driven by GH-induced excessive bone turnover that occurs rapidly with exposure to pathologic levels of GH. This is the first report describing the morphology of femoral SCB in states of excess GH, showing significant microstructural changes. Specifically, male bGH mice exhibited significant decreases in BV/TV, Tb.Th, and BMD, whereas female bGH mice showed reductions in Tb.Th only. Both male and female bGH mice showed increased resorption activity in the femoral SCB, evidenced by tartrate-resistant acid phosphatase staining, which can potentially affect the progression of OA.

Ectopic chondrogenesis was detected in several joint tissues, including the synovium and the ligaments. Ectopic chondrogenesis in joint tissues is normally not observed in injury-related or primary OA. It is possible that excess GH or IGF-1 stimulates chondrogenic differentiation of precursor cells in the synovium or ligaments. Ectopic chondrogenesis in the synovium has been observed in patients after total knee arthroplasty, leading to pseudogout.³⁴ It often occurs in tendons and ligaments after injury or tendon/ligament degenerative disorders.³⁵ Because it leads to calcification in these tissues, similar to that seen in the growth plate during endochondral bone formation, ectopic

chondrogenesis can become a painful event. Therefore, these findings indicate that ectopic chondrogenesis observed in bGH mice may contribute to increased pain.

Osteophytosis is common in acromegalic arthropathy. Osteophyte formation is primarily a process of neo-chondrogenesis of mesenchymal stem cells found in the periosteum and bone-cartilage junction, and can be stimulated by growth factors secreted from macrophages of the synovial membrane.³⁶ Ectopic chondrogenesis, which was detected in all joint tissues, can potentially develop to osteophytes. Previous studies have shown that IGF-1 (which is extremely elevated in the bGH mice) increases chondrogenesis in a dose-dependent manner.^{37,38} Thus, it is possible that the high levels of IGF-1 promoted osteophytosis in the bGH mice.

Chondrocytes in OA cartilage show an aberrant expression of matrix-degrading enzymes, such as MMP13, aggrecanases, and inflammatory markers. One explanation for the catabolic phenotype of OA chondrocytes is related to cytokine-mediated stimulation of AC chondrocytes to secrete those enzymes and initiate a vicious cycle of matrix degradation.³⁹ Another possibility is that AC chondrocytes differentiate and become hypertrophic chondrocytes, a state typified by acquisition of an autolytic phenotype, where chondrocytes destroy their surrounding cartilage, allowing calcification and ossification (similar to the hypertrophic and terminal differentiation events occurring in the growth plate^{40,41}). Indeed, pathologic calcification of the AC was found to be associated with increased expression of chondrocyte hypertrophy markers.⁴² There are several markers of hypertrophic chondrocytes; the most recognized are type X collagen and MMP13.^{43,44} Notably, however, increases in MMP13 protein levels do not necessarily pertain to increased enzymatic activity. Relevant to the current study, both elevated expression of inflammatory markers (MMP13, iNOS, and NLRP3) and high levels of type X collagen were found by immunohistochemistry. Increases in type X collagen were associated with increased expression of RUNX2 transcription factor in the AC of bGH mice, as was shown in an experimental mouse OA model.⁴⁵ Accordingly, a previous study has shown that RUNX2 was up-regulated in fibrillated OA cartilage and colocalized with MMP13 in clusters of chondrocytes,⁴⁶ whereas chondrocyte-specific deletion of RUNX2 could partially rescue injury-induced OA.⁴⁷ On the other hand, the levels of SOX9 transcription factor were significantly reduced in bGH AC compared with WT mice. SOX9 is essential for counteracting chondrocyte dedifferentiation or osteoblast redifferentiation process²³ and plays significant roles in repressing A disintegrin and metalloproteinase with thrombospondin motifs during OA cartilage degradation.⁴⁸ Finally, SOX9 was shown to inhibit IL-1b-induced inflammatory response.⁴⁹ Thus, decreases in SOX9 expression in the bGH AC may partially underlay the enhanced inflammatory response in these mice. Overall, both chondrocyte hypertrophy and the

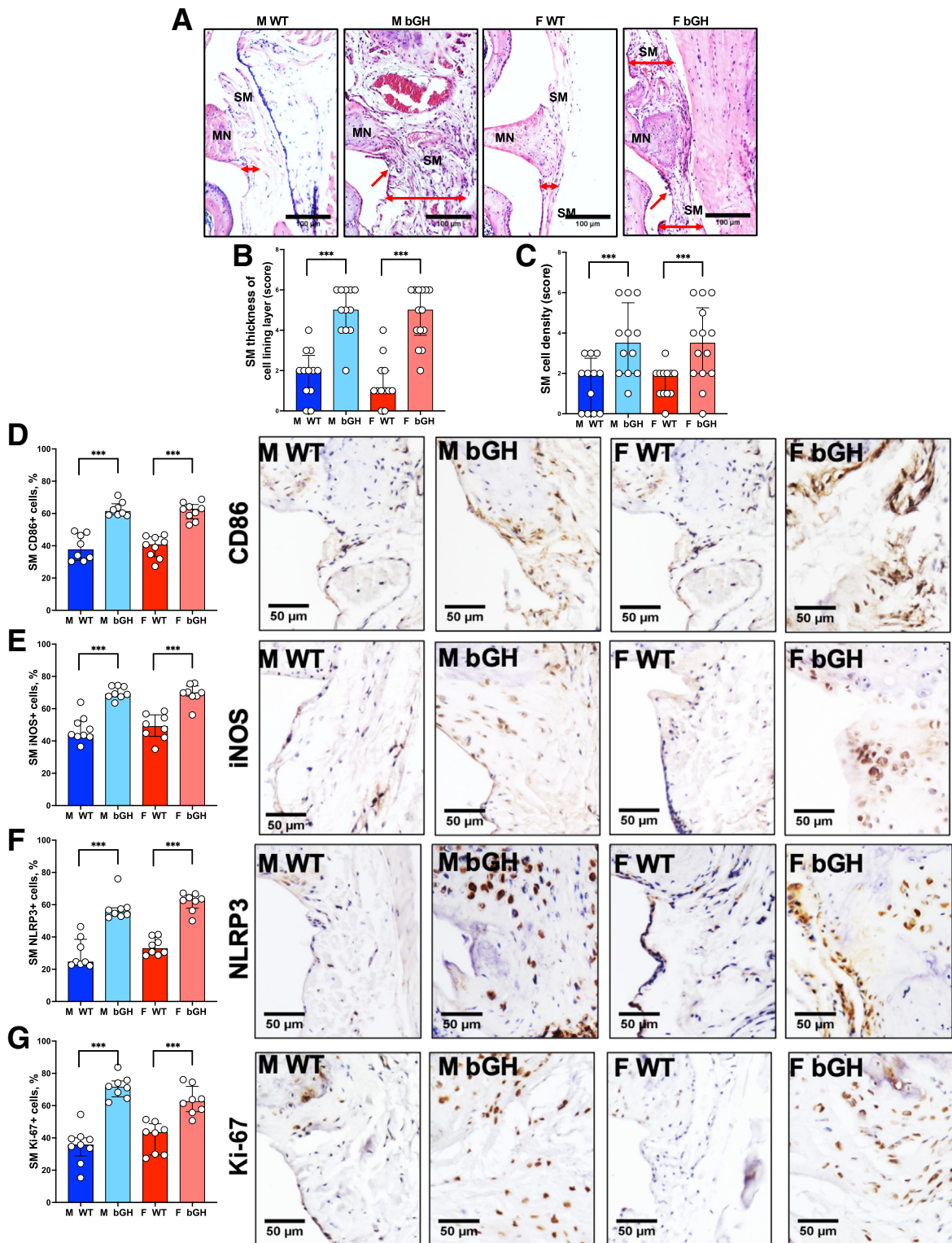


Figure 6 Excess growth hormone (GH) promotes synovitis. **A:** Synovitis was scored from hematoxylin and eosin–stained sections. **Red arrows** point to the synovial membrane (SM), and **double-headed red arrows** define the thickness of the SM. **B** and **C:** Thickness of the synovial membrane lining cell layer (**B**) and synovial membrane cell density (**C**) was scored according to Osteoarthritis Research Society International scoring system [male (M) wild type (WT), $n = 12$; M bovine GH (bGH), $n = 12$; female (F) WT, $n = 12$; and F bGH, $n = 14$]. Expression of inflammatory markers was assessed by immunohistochemistry. **D–G:** Presented are percentages of positive cells in the medial synovial membrane alongside representative immunohistochemistry images to the following markers: CD86 ($n = 5$ in each group; **D**), inducible nitric oxide synthase (iNOS; $n = 5$ in each group; **E**), nucleotide oligomerization domain (NOD)–like receptor–pyrin domain-containing 3 (NLRP3; M WT, $n = 8$; M bGH, $n = 8$; F WT, $n = 8$; and F bGH, $n = 8$; **F**), and Ki-67 (M WT, $n = 9$; M bGH, $n = 8$; F WT, $n = 8$; and F bGH, $n = 8$; **G**). Data presented as median \pm IQR (**B–G**). $***P < 0.001$. Scale bars: 100 μm (**A**); 50 μm (**D–G**). MN, meniscus.

activation of catabolic events in chondrocytes likely contribute to the development of OA in response to chronic excess GH.

Previous studies have shown an association between aberrant growth plate dynamics and development of OA during aging in a spontaneous model of OA (STR/Ort mouse).⁵⁰ Accordingly, canine studies have shown that femoral lengthening by 30% led to knee AC damage.⁵¹ More importantly, the current study showed that the bGH mice displayed an excessive growth phenotype with increased bone growth rates, growth plate widths, and chondrocyte proliferation compared with age-matched WT mice. Therefore, it is possible that the altered growth phenotype in bGH mice contributes to the development of OA in aging bGH mice. The mechanisms by which accelerated growth in bGH mice affects OA development are yet to be defined, but they need to be taken in consideration when using the bGH mouse as a model for acromegalic arthropathy.

The impact of excess GH on systemic or synovial joint inflammation was not tested directly. Numerous studies reported anti-inflammatory effects of GH/IGF-1.⁵² In a rabbit model of OA, IGF-1 delivery inhibited inflammation mediated by NF- κ B and prevented chondrocyte apoptosis and cartilage degradation.⁵³ However, subjects with acromegaly were shown to exhibit an activation of the innate immune system and a proinflammatory state with low-grade inflammation.^{54,55} The innate immune system recognizes damage-associated molecular patterns produced during AC damage. Prolonged and dysregulated activation of damage-associated molecular pattern–induced inflammation can be destructive, and it has been implicated in the chronic inflammation observed in OA.^{56,57} Activated macrophages in the synovium of OA joints contribute to cartilage breakdown and osteophytosis⁵⁸ by secreting cytokines, such as IL-1 β , lymphotoxin-a, as well as MMPs,^{36,59} and other inflammatory markers, such as iNOS⁵⁹ and CD86.⁶⁰ Ki-67, a cell proliferation marker, highly expressed in inflamed synovial membrane,^{61,62} was also up-regulated in the synovial membrane of bGH mice. These findings suggest a relationship between excess GH and chronic inflammation in knee joints of bGH mice. The exact mechanisms of how excess GH causes chronic inflammation in knee joints, however, still need to be established.

In summary, the current study showed that excess GH affects all tissues of the joint, leading to increased SCB remodeling with increased osteoclast number on bone surface, promotion of hypertrophy of the articular cartilage chondrocytes that increase their expression of inflammatory markers, induction of ectopic chondrogenesis in the meniscus and synovial membrane, and activation of resident macrophages that likely aggravate disease progression. These results are clinically relevant to acromegaly, which is a rare disease with excess GH, requiring a lifelong management of severe comorbidities, including arthropathy. In patients with acromegaly, IGF-1

levels before surgery/therapy range between 2.34 and 9.2 SD score.^{63,64} Unfortunately, there is often a delay of 7 to 10 years between the appearance of the initial symptoms and diagnosis; thus, early treatments of arthropathy and arthralgia are important for delaying disease progression and achieving successful outcomes. It is possible that targeting synovitis, chondrocyte hypertrophy, and ectopic chondrogenesis in subjects with acromegaly will provide an effective therapy.

Author Contributions

S.Y. conceptualized the study; S.Y. acquired funding; R.R.R. and S.Y. analyzed data; S.B.P., G.Y., M.D., B.M., and J.L.G. conducted experiments; R.R.R. performed statistical analyses; J.J.K. and S.D.O. obtained resources (bovine growth hormone transgenic mice); S.B.P. and S.Y. wrote the manuscript; and S.Y. and T.K. reviewed and edited the manuscript. All authors discussed the results and approved the final version of the manuscript. S.Y. is the guarantor of this work and, as such, had full access to all the data in the study and takes responsibility for the integrity of the data and the accuracy of the data analysis.

Supplemental Data

Supplemental material for this article can be found at <http://doi.org/10.1016/j.ajpath.2023.02.010>.

References

1. Claessen KM, Mazziotti G, Biermasz NR, Giustina A: Bone and joint disorders in acromegaly. *Neuroendocrinology* 2016, 103:86–95
2. Wassenaar MJ, Biermasz NR, Bijsterbosch J, Pereira AM, Meulenbelt I, Smit JW, Roelfsema F, Kroon HM, Romijn JA, Kloppenburg M: Arthropathy in long-term cured acromegaly is characterised by osteophytes without joint space narrowing: a comparison with generalised osteoarthritis. *Ann Rheum Dis* 2011, 70:320–325
3. Colao A, Marzullo P, Vallone G, Marino V, Annecchino M, Ferone D, De Brasi D, Scarpa R, Oriente P, Lombardi G: Reversibility of joint thickening in acromegalic patients: an ultrasonography study. *J Clin Endocrinol Metab* 1998, 83:2121–2125
4. Man GS, Mologhianu G: Osteoarthritis pathogenesis - a complex process that involves the entire joint. *J Med Life* 2014, 7:37–41
5. Akkiraju H, Nohe A: Role of chondrocytes in cartilage formation, progression of osteoarthritis and cartilage regeneration. *J Dev Biol* 2015, 3:177–192
6. Heijink A, Gomoll AH, Madry H, Drobnic M, Filardo G, Espregueira-Mendes J, Van Dijk CN: Biomechanical considerations in the pathogenesis of osteoarthritis of the knee. *Knee Surg Sports Traumatol Arthrosc* 2012, 20:423–435
7. Chrisman OD: The effect of growth hormone on established cartilage lesions: a presidential address to the Association of Bone and Joint Surgeons, 1974. *Clin Orthop Relat Res* 1975:232–238
8. Maor G, Hochberg Z, von der Mark K, Heinegard D, Silbermann M: Human growth hormone enhances chondrogenesis and osteogenesis in a tissue culture system of chondroprogenitor cells. *Endocrinology* 1989, 125:1239–1245

9. Tsukazaki T, Matsumoto T, Enomoto H, Usa T, Ohtsuru A, Namba H, Iwasaki K, Yamashita S: Growth hormone directly and indirectly stimulates articular chondrocyte cell growth. *Osteoarthritis Cartilage* 1994, 2:259–267
10. Fernandez-Criado C, Martos-Rodriguez A, Santos-Alvarez I, Garcia-Ruiz JP, Delgado-Baeza E: The fate of chondrocyte in osteoarthritic cartilage of transgenic mice expressing bovine GH. *Osteoarthritis Cartilage* 2004, 12:543–551
11. Munoz-Guerra MF, Delgado-Baeza E, Sanchez-Hernandez JJ, Garcia-Ruiz JP: Chondrocyte cloning in aging and osteoarthritis of the hip cartilage: morphometric analysis in transgenic mice expressing bovine growth hormone. *Acta Orthop Scand* 2004, 75:210–216
12. Ogueta S, Olazabal I, Santos I, Delgado-Baeza E, Garcia-Ruiz JP: Transgenic mice expressing bovine GH develop arthritic disorder and self-antibodies. *J Endocrinol* 2000, 165:321–328
13. Kaps M, Moura AS, Safranski TJ, Lamberson WR: Components of growth in mice hemizygous for a MT/bGH transgene. *J Anim Sci* 1999, 77:1148–1154
14. Chaplan SR, Bach FW, Pogrel JW, Chung JM, Yaksh TL: Quantitative assessment of tactile allodynia in the rat paw. *J Neurosci Methods* 1994, 53:55–63
15. Bouxsein ML, Boyd SK, Christiansen BA, Guldberg RE, Jepsen KJ, Muller R: Guidelines for assessment of bone microstructure in rodents using micro-computed tomography. *J Bone Miner Res* 2010, 25:1468–1486
16. Glasson SS, Chambers MG, Van Den Berg WB, Little CB: The OARSI histopathology initiative - recommendations for histological assessments of osteoarthritis in the mouse. *Osteoarthr Cartil* 2010, 18(Suppl 3):S17–S23
17. Kraus VB, Huebner JL, DeGroot J, Bendele A: The OARSI histopathology initiative - recommendations for histological assessments of osteoarthritis in the guinea pig. *Osteoarthr Cartil* 2010, 18(Suppl 3):S35–S52
18. Kaneko H, Ishijima M, Futami I, Tomikawa-Ichikawa N, Kosaki K, Sadatsuki R, Yamada Y, Kurosawa H, Kaneko K, Arikawa-Hirasawa E: Synovial perlecan is required for osteophyte formation in knee osteoarthritis. *Matrix Biol* 2013, 32:178–187
19. Chambers MG, Bayliss MT, Mason RM: Chondrocyte cytokine and growth factor expression in murine osteoarthritis. *Osteoarthr Cartil* 1997, 5:301–308
20. Pelletier JP, Martel-Pelletier J, Ghandur-Mnaimneh L, Howell DS, Woessner JF Jr: Role of synovial membrane inflammation in cartilage matrix breakdown in the Pond-Nuki dog model of osteoarthritis. *Arthritis Rheum* 1985, 28:554–561
21. Grote CW, Mackay MJ, Liu X, Lu Q, Wang J: A modified comprehensive grading system for murine knee osteoarthritis: scoring the whole joint as an organ. *bioRxiv* 2021, [Preprint] doi: <https://doi.org/10.1101/2021.05.05.442864>
22. Yoav Benjamini YH: Controlling the false discovery rate: a practical and powerful approach to multiple testing. *J R Stat Soc Ser B Methodol* 1995, 57:289–300
23. Haseeb A, Kc R, Angelozzi M, de Charleroy C, Rux D, Tower RJ, Yao L, Pellegrino da Silva R, Pacifici M, Qin L, Lefebvre V: SOX9 keeps growth plates and articular cartilage healthy by inhibiting chondrocyte dedifferentiation/osteoblastic redifferentiation. *Proc Natl Acad Sci U S A* 2021, 118:e2019152118
24. Kapoor M, Martel-Pelletier J, Lajeunesse D, Pelletier JP, Fahmi H: Role of proinflammatory cytokines in the pathophysiology of osteoarthritis. *Nat Rev Rheumatol* 2011, 7:33–42
25. Burrage PS, Mix KS, Brinckerhoff CE: Matrix metalloproteinases: role in arthritis. *Front Biosci* 2006, 11:529–543
26. Vuolteenaho K, Moilanen T, Al-Saffar N, Knowles RG, Moilanen E: Regulation of the nitric oxide production resulting from the glucocorticoid-insensitive expression of iNOS in human osteoarthritic cartilage. *Osteoarthr Cartil* 2001, 9:597–605
27. Jin C, Frayssinet P, Pelker R, Cwirka D, Hu B, Vignery A, Eisenbarth SC, Flavell RA: NLRP3 inflammasome plays a critical role in the pathogenesis of hydroxyapatite-associated arthropathy. *Proc Natl Acad Sci U S A* 2011, 108:14867–14872
28. Hu Q, Ecker M: Overview of MMP-13 as a promising target for the treatment of osteoarthritis. *Int J Mol Sci* 2021, 22:1742
29. Chesnokova V, Zonis S, Apostolou A, Estrada HQ, Knott S, Wawrowsky K, Michelsen K, Ben-Shlomo A, Barrett R, Gorbunova V, Karalis K, Melmed S: Local non-pituitary growth hormone is induced with aging and facilitates epithelial damage. *Cell Rep* 2021, 37:110068
30. Piotrowska K, Sluczanska-Glabowska S, Kucia M, Bartke A, Laszczynska M, Ratajczak MZ: Histological changes of testes in growth hormone transgenic mice with high plasma level of GH and insulin-like growth factor-1. *Folia Histochem Cytobiol* 2015, 53:249–258
31. Westbrook R, Bonkowski MS, Strader AD, Bartke A: Alterations in oxygen consumption, respiratory quotient, and heat production in long-lived GHRKO and Ames dwarf mice, and short-lived bGH transgenic mice. *J Gerontol A Biol Sci Med Sci* 2009, 64:443–451
32. Hu W, Chen Y, Dou C, Dong S: Microenvironment in subchondral bone: predominant regulator for the treatment of osteoarthritis. *Ann Rheum Dis* 2021, 80:413–422
33. Lacourt M, Gao C, Li A, Girard C, Beauchamp G, Henderson JE, Laverty S: Relationship between cartilage and subchondral bone lesions in repetitive impact trauma-induced equine osteoarthritis. *Osteoarthr Cartil* 2012, 20:572–583
34. Sato R, Nakano S, Takasago T, Nakamura M, Kashima M, Chikawa T, Hamada D, Goto T, Sairyu K: Chondrogenesis in the synovial tissue is associated with the onset of pseudogout after total knee arthroplasty. *Arthroplast Today* 2016, 2:101–104
35. Lui PP, Chan LS, Cheuk YC, Lee YW, Chan KM: Expression of bone morphogenetic protein-2 in the chondrogenic and ossifying sites of calcific tendinopathy and traumatic tendon injury rat models. *J Orthop Surg Res* 2009, 4:27
36. van Lent PL, Blom AB, van der Kraan P, Holthuysen AE, Vitters E, van Rooijen N, Smeets RL, Nabbe KC, van den Berg WB: Crucial role of synovial lining macrophages in the promotion of transforming growth factor beta-mediated osteophyte formation. *Arthritis Rheum* 2004, 50:103–111
37. Mierisch CM, Anderson PC, Balian G, Diduch DR: Treatment with insulin-like growth factor-1 increases chondrogenesis by periosteum in vitro. *Connect Tissue Res* 2002, 43:559–568
38. Fukumoto T, Sperling JW, Sanyal A, Fitzsimmons JS, Reinholz GG, Conover CA, O'Driscoll SW: Combined effects of insulin-like growth factor-1 and transforming growth factor-beta1 on periosteal mesenchymal cells during chondrogenesis in vitro. *Osteoarthr Cartil* 2003, 11:55–64
39. Loeser RF: Age-related changes in the musculoskeletal system and the development of osteoarthritis. *Clin Geriatr Med* 2010, 26:371–386
40. Dreier R: Hypertrophic differentiation of chondrocytes in osteoarthritis: the developmental aspect of degenerative joint disorders. *Arthritis Res Ther* 2010, 12:216
41. von der Mark K, Kirsch T, Nerlich A, Kuss A, Weseloh G, Gluckert K, Stoss H: Type X collagen synthesis in human osteoarthritic cartilage: indication of chondrocyte hypertrophy. *Arthritis Rheum* 1992, 35:806–811
42. Fuerst M, Bertrand J, Lammers L, Dreier R, Echtermeyer F, Nitschke Y, Rutsch F, Schafer FK, Niggemeyer O, Steinhagen J, Lohmann CH, Pap T, Ruther W: Calcification of articular cartilage in human osteoarthritis. *Arthritis Rheum* 2009, 60:2694–2703
43. Alvarez J, Balbin M, Santos F, Fernandez M, Ferrando S, Lopez JM: Different bone growth rates are associated with changes in the expression pattern of types II and X collagens and collagenase 3 in proximal growth plates of the rat tibia. *J Bone Miner Res* 2000, 15:82–94
44. Kirsch T, von der Mark K: Remodelling of collagen types I, II and X and calcification of human fetal cartilage. *Bone Miner* 1992, 18:107–117
45. Kamekura S, Kawasaki Y, Hoshi K, Shimoaka T, Chikuda H, Maruyama Z, Komori T, Sato S, Takeda S, Karsenty G, Nakamura K,

- Chung UI, Kawaguchi H: Contribution of runt-related transcription factor 2 to the pathogenesis of osteoarthritis in mice after induction of knee joint instability. *Arthritis Rheum* 2006, 54:2462–2470
46. Wang X, Manner PA, Horner A, Shum L, Tuan RS, Nuckolls GH: Regulation of MMP-13 expression by RUNX2 and FGF2 in osteoarthritic cartilage. *Osteoarthr Cartil* 2004, 12:963–973
 47. Liao L, Zhang S, Gu J, Takarada T, Yoneda Y, Huang J, Zhao L, Oh CD, Li J, Wang B, Wang M, Chen D: Deletion of Runx2 in articular chondrocytes decelerates the progression of DMM-induced osteoarthritis in adult mice. *Sci Rep* 2017, 7:2371
 48. Zhang Q, Ji Q, Wang X, Kang L, Fu Y, Yin Y, Li Z, Liu Y, Xu X, Wang Y: SOX9 is a regulator of ADAMTSs-induced cartilage degeneration at the early stage of human osteoarthritis. *Osteoarthr Cartil* 2015, 23:2259–2268
 49. Ouyang Y, Wang W, Tu B, Zhu Y, Fan C, Li Y: Overexpression of SOX9 alleviates the progression of human osteoarthritis in vitro and in vivo. *Drug Des Devel Ther* 2019, 13:2833–2842
 50. Staines KA, Madi K, Mirczuk SM, Parker S, Burleigh A, Poulet B, Hopkinson M, Bodey AJ, Fowkes RC, Farquharson C, Lee PD, Pitsillides AA: Endochondral growth defect and deployment of transient chondrocyte behaviors underlie osteoarthritis onset in a natural murine model. *Arthritis Rheumatol* 2016, 68:880–891
 51. Stanitski DF, Rossman K, Torosian M: The effect of femoral lengthening on knee articular cartilage: the role of apparatus extension across the joint. *J Pediatr Orthop* 1996, 16:151–154
 52. Deepak D, Daousi C, Javadpour M, Clark D, Pery Y, Pinkney J, Macfarlane IA: The influence of growth hormone replacement on peripheral inflammatory and cardiovascular risk markers in adults with severe growth hormone deficiency. *Growth Horm IGF Res* 2010, 20:220–225
 53. Hossain MA, Adithan A, Alam MJ, Kopalli SR, Kim B, Kang CW, Hwang KC, Kim JH: IGF-1 facilitates cartilage reconstruction by regulating PI3K/AKT, MAPK, and NF- κ B signaling in rabbit osteoarthritis. *J Inflamm Res* 2021, 14:3555–3568
 54. Arikan S, Bahceci M, Tuzcu A, Gokalp D: Serum tumour necrosis factor-alpha and interleukin-8 levels in acromegalic patients: acromegaly may be associated with moderate inflammation. *Clin Endocrinol (Oxf)* 2009, 70:498–499
 55. Wolters TLC, van der Heijden C, van Leeuwen N, Hijmans-Kersten BTP, Netea MG, Smit JW, Thijssen DHJ, Hermus A, Riksen NP, Netea-Maier R: Persistent inflammation and endothelial dysfunction in patients with treated acromegaly. *Endocr Connect* 2019, 8:1553–1567
 56. Orlowsky EW, Kraus VB: The role of innate immunity in osteoarthritis: when our first line of defense goes on the offensive. *J Rheumatol* 2015, 42:363–371
 57. Sokolove J, Lepus CM: Role of inflammation in the pathogenesis of osteoarthritis: latest findings and interpretations. *Ther Adv Musculoskelet Dis* 2013, 5:77–94
 58. Blom AB, van Lent PL, Holthuysen AE, van der Kraan PM, Roth J, van Rooijen N, van den Berg WB: Synovial lining macrophages mediate osteophyte formation during experimental osteoarthritis. *Osteoarthr Cartil* 2004, 12:627–635
 59. Blom AB, van Lent PL, Libregts S, Holthuysen AE, van der Kraan PM, van Rooijen N, van den Berg WB: Crucial role of macrophages in matrix metalloproteinase-mediated cartilage destruction during experimental osteoarthritis: involvement of matrix metalloproteinase 3. *Arthritis Rheum* 2007, 56:147–157
 60. Hock BD, O'Donnell JL, Taylor K, Steinkasserer A, McKenzie JL, Rothwell AG, Summers KL: Levels of the soluble forms of CD80, CD86, and CD83 are elevated in the synovial fluid of rheumatoid arthritis patients. *Tissue Antigens* 2006, 67:57–60
 61. Cai L, Li CM, Tang WJ, Liu MM, Chen WN, Qiu YY, Li R: Therapeutic effect of penta-acetyl geniposide on adjuvant-induced arthritis in rats: involvement of inducing synovial apoptosis and inhibiting NF- κ B signal pathway. *Inflammation* 2018, 41:2184–2195
 62. Pessler F, Ogdie A, Diaz-Torne C, Dai L, Yu X, Einhorn E, Gay S, Schumacher HR: Subintimal Ki-67 as a synovial tissue biomarker for inflammatory arthropathies. *Ann Rheum Dis* 2008, 67:162–167
 63. Subbarayan SK, Fleseriu M, Gordon MB, Brzana JA, Kennedy L, Faiman C, Hatipoglu BA, Prayson RA, Delashaw JB, Weil RJ, Hamrahian AH: Serum IGF-1 in the diagnosis of acromegaly and the profile of patients with elevated IGF-1 but normal glucose-suppressed growth hormone. *Endocr Pract* 2012, 18:817–825
 64. Ho KY, Weissberger AJ: Characterization of 24-hour growth hormone secretion in acromegaly: implications for diagnosis and therapy. *Clin Endocrinol (Oxf)* 1994, 41:75–83